Flying Bird Detection and Hazard Assessment for Avian Radar System

Weishi Chen, Ph.D.[1]; Huansheng Ning, Ph.D.[2]; and Jing Li, Ph.D.[3]

Downloaded from ascelibrary.org by University of Science & Technology Beijing on 07/07/16. Copyright ASCE. For personal use only; all rights reserved.

Abstract: An airport-based avian radar system is an effective technical means for bird-aircraft strike hazard (BASH) avoidance. Three existing systems are surveyed, including Merlin Avian Radar System, Accipiter Avian Radar System, and Beihang Experimental Avian Radar System. Two critical technologies for Beihang experimental system are introduced: flying bird target detecting and tracking algorithm and BASH assessment. The algorithm consists of five steps: background subtraction, clutter suppression, measurement extraction, multitarget tracking, and data overlay. The multitarget tracking algorithm is tested against simulated data. The overall approach is applied on a set of horizontal scanning plane position indicator (PPI) radar images. A BASH assessment model is established by an analytic hierarchy process (AHP), considering two factors of the current states of flying birds and aircraft. Using the BASH assessment model, an application example at Nanyang Airport is described, in detail. Finally, some development trend of critical technologies for airport-based avian radar system is given.
DOI: 10.1061/(ASCE)AS.1943-5525.0000131. © *2012 American Society of Civil Engineers.*

CE Database subject headings: Radar; Aircraft; Wildlife; Safety; Assessment.

Author keywords: BASH; Radar; Tracking; Assessment; AHP.

Introduction

The heroic ditching in the Hudson River of U.S. Airway's Flight 1549, following multiple bird strikes with Canada geese on January 15, 2009, has increased public awareness of bird-aircraft strike hazards (BASH) and has focused attention on new tools, such as avian radar, to help further improve aviation safety. Reports have suggested that had avian radars been deployed at LaGuardia Airport, this bird-strike could have been avoided (Nohara 2009a). Indeed, birds pose a threat to aviation safety and cost air carriers and insurance companies approximately $2 billion each year (Klope et al. 2009). More than 60% of these collisions occur within the confines of airfields, in which an avian radar system can be used to provide air operations personnel with greatly improved bird situational awareness to reduce bird hazards around airports for improved safety.

Over the past 40 years, airport-based avian radar systems were an interdisciplinary subject attracting interests of researchers and consultants over the world. Some excellent products have been developed and applied in many civil or military airports. Commercial secrets as they are, however, limit the reporting of critical technical details of these systems. In this paper, two critical technologies for the Beihang Experimental Avian Radar System (BHEARS) are explained in detail, including the flying bird detection and tracking algorithm and the BASH assessment model.

[1]Postdoctoral, School of Electronics and Information Engineering, Beihang Univ., Beijing 100191, China (corresponding author). E-mail: wishchen@ee.buaa.edu.cn

[2]Associate Professor, School of Electronics and Information Engineering, Beihang Univ., Beijing 100191, China.

[3]Senior Engineer, China Academy of Civil Aviation Science and Technology, Beijing 100028, China.

Note. This manuscript was submitted on December 7, 2009; approved on May 10, 2011; published online on May 12, 2011. Discussion period open until September 1, 2012; separate discussions must be submitted for individual papers. This paper is part of the ***Journal of Aerospace Engineering***, Vol. 25, No. 2, April 1, 2012. ©ASCE, ISSN 0893-1321/2012/2-246–255/$25.00.

The paper is organized as follows: an overview of three existing airport-based avian radar systems, including the Merlin system, Accipiter system, and Beihang experimental system; two critical technologies for BHEARS are then introduced in detail; after describing the flying bird target detecting and tracking algorithm, the tracking algorithm is tested by simulated data, and the overall technique is applied to live plane position indicator (PPI) radar images; the BASH assessment model is analyzed, and results obtained against ground-truth data collected at Nanyang Airport are reported, showing the performance achievable in a practical application of the experimental system. Some conclusions and future work close the paper.

Existing Airport-Based Avian Radar Systems

At most airports, visual observations are the primary source of real-time bird situational awareness and are reliable only during the daylight hours at relatively short distances of up to a few hundred meters (Nohara 2009b). An airport-based avian radar system acts as a powerful force multiplier to wildlife management personnel at the airport by providing wide-area, all-weather, day-night automatic situational awareness. In this section, three existing airport-based avian radar systems are introduced.

Merlin Avian Radar System

The Merlin Avian Radar System is developed by DeTect, Inc., (Panama City, FL). Different models of the system are utilized in many civil and military airports all over the world. For example, the Model XS2530m is installed at the Dover Air Force Base in Delaware, supporting military airlift. For affordability, two marine radars are always used. The system utilizes a two-radar configuration consisting of a vertically scanned *X*-band radar and a horizontally scanned *S*-band radar. The two radars use different frequencies and therefore, can be operated simultaneously without interference, collecting data in both the vertical and horizontal directions

continually with no data gaps. In the horizontal position, the radar sends out a fan-shaped beam (approximately 20°), which is mechanically rotated through 360° around its location, returning *x*-*y* coordinates for targets detected within its range. For vertical operation, the radar is tilted up 90° on its side operating in a windmill-type manner scanning horizon-to-horizon through the vertical plane. In this orientation, the radar scans a vertical slice through the atmosphere collecting data on the target altitude across the scan width providing *y*-*z* location data.

Depending on the radar power selected, these systems can reliably detect and track small birds (e.g., sparrows) up to 1,524 m (5,000 ft) vertically and out to 3.7–5.6 km [2–3 nautical miles (nmi)] horizontally. Two marine radar monitors show raw radar imagery for the horizontally-scanned *S*-band and vertically-scanned *X*-band radars. A stationary background includes clutter from trees, buildings, and radar side-lobe interference. Radar data processing software detects and tracks bird targets, displaying the information on computer monitors. The respective horizontal and vertical PPI radar images are processed, and the results are shown on two separate displays. In addition, processed bird tracks are classified by the software into bird size categories: small, medium, and large. Bird distribution around the airport is summarized on the basis of bird information stored in the database for a long period, which is helpful to wildlife management at airports.

Accipiter Avian Radar System

The Accipiter Avian Radar System (Nohara et al. 2007) is developed by Sicom Systems Ltd., Canada as a low-cost alternative for real-time BASH applications at airports. To obtain three-dimensional (3D) target information, a modified parabolic antenna is adopted to provide altitude data attributed to its 4° narrow beam. The antenna can be inclined in elevation to match the volume coverage needed during take-off and landing. The radar system is housed in a field-deployable trailer containing the radar, the radar controls, the radar processor, and a global positioning system (GPS). The antenna is mounted on the roof of a trailer or on a cart configuration with an adjustable elevation angle. Elevation is typically set between 0 and 30° above the horizon. A digital radar processor interfaces to the radar and is responsible for all real-time postprocessing, including detection processing, track processing, and display processing.

Beihang Experimental Avian Radar System

With the cooperation of the China Academy of Civil Aviation Science and Technology, BHEARS was developed by Beihang University and serves as a platform for further improvements (Ning et al. 2010). Fig. 1(a) shows a field experiment at an airport. Fig. 1(b) illustrates the overall architecture of the experimental system. A Furuno Model 1941 Mark-2 *X*-band radar with 6 kW power is operated in alternating horizontal and vertical positions for the survey. The 1.2-m T-bar antenna (slotted waveguide antenna array) rotates at 24 RPM with a 20° elevation beam width. The PPI radar images collected by the capture card every 2.5 s are stored in an avian radar image database and processed by a self-developed algorithm in real-time software, which will be subsequently discussed in detail. The extracted bird information is processed by the BASH assessment model, and the assessment value is calculated and shown on a display, warning the operators to take appropriate measures. This model will be particularly explained subsequently. The maximum detection range varies with the bird target size. Depending on their radar cross sections (RCS), large

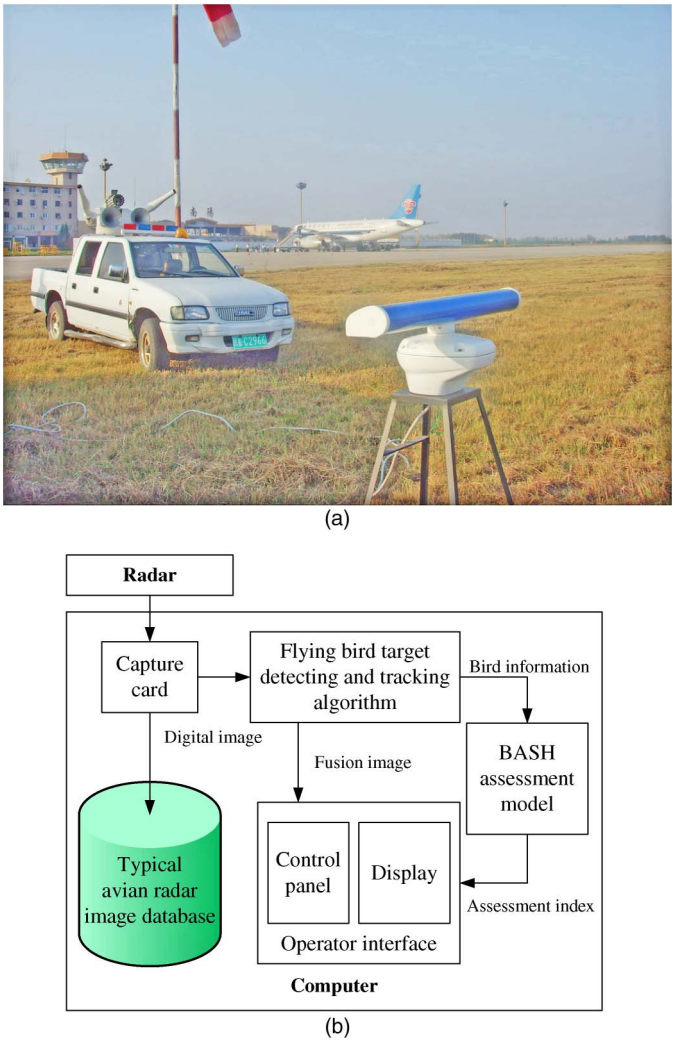

Fig. 1. Beihang experimental avian radar system: (a) field experiment at airport (image by W. Chen); (b) system architecture

individual birds, such as swans, can be tracked several miles out, whereas flocks can be tracked to 10 nmi and beyond.

Flying Bird Target Detecting and Tracking Algorithm

The flying bird target detecting and tracking algorithm, whose flowchart is illustrated in Fig. 2, is the significant technology for BHEARS. The algorithm consists of five steps: background subtraction, clutter suppression, measurements extraction, multitarget tracking, and data overlay. The first three steps complete the task of detection, and the remaining two realize the functions of tracking and display. In this section, the five parts will be analyzed, in detail, especially the parts of clutter suppression and multitarget tracking. Traditional clutter suppression algorithms tried to detect the target at each scan depending on comparison of gray scales of the targets and background (Ning et al. 2010). The algorithms worked well when targets are brighter than the background but performed poorly for dim targets when clutters are even stronger. Actually, gray value information is not enough, and a spatial characteristic could be utilized for such situations. In PPI radar images, marginal echoes of nonrigid objects (e.g., wood, farmland, and buildings) mapped in the image are not stable, so clutters primarily appear at the edges of these objects. In this paper, the target will be distinguished from the clutter according to its spatial distribution

J. Aerosp. Eng., 2012, 25(2): 246-255

Downloaded from ascelibrary.org by University of Science & Technology Beijing on 07/07/16. Copyright ASCE. For personal use only; all rights reserved.

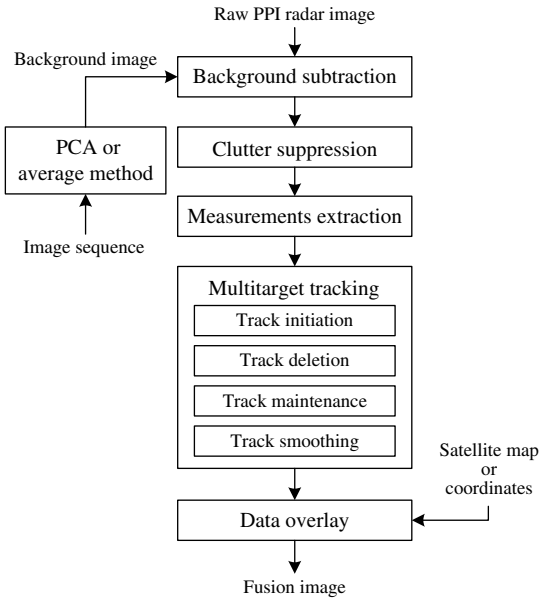

Fig. 2. Flowchart of a flying bird target detecting and tracking algorithm

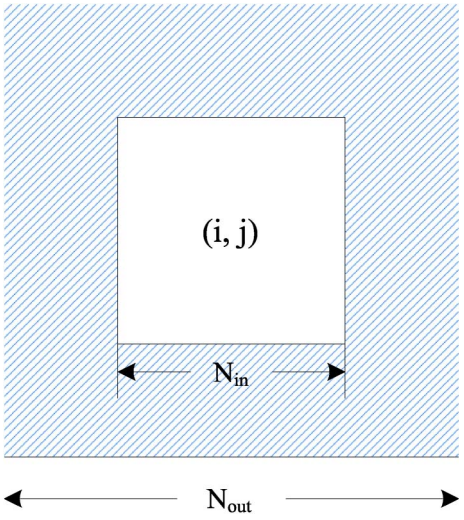

Fig. 3. Target detection mask architecture

feature. In addition, the continuity characteristic of target motion in sequential scans is utilized for multitarget tracking. Following the particle-filtering-based algorithm for data association used before, a new approach with formulation of probabilistic stochastic process models is proposed for tracking an unknown number of targets. These stochastic processes include the birth, maintenance, and death of each target and the combination of different possible associated events, which will be enumerated in the subsection of track maintenance.

Background Subtraction

Background subtraction is the first step in bird target's detection. Therefore, it is essential to construct an adaptive background image. Two approaches can be used for background construction: principal component analysis (PCA) and average method. The PCA algorithm focuses on the computation of several principal components, which will be uncorrelated and will maximize the variance accounted for in the original variables. In this case, the original variables are a set of PPI radar images, and the background is obtained by computing the maximum principal component. Because the background changes with time because of variations of the surrounding environment, the background image is usually updated as a time averaged version of the input image sequence periodically for engineering applications.

Clutter Suppression

After background subtraction, there is still a large quantity of clutter in the image, especially distributed randomly around the edge of the background, so further clutter suppression is necessary. Threshold calculation is the basic step for clutter suppression because if the thresholds are too high, no targets will be seen. If the thresholds are too low, the system will be swamped with false alarms from clutter. To identify a detection threshold for candidate targets, a fixed value is the simplest, but does not provide any dynamic response to changes in the input images (Beckwith 2005). However, the background-edge clutter is usually caused by unstable echoes from the nonrigid objects. Compared with clutter, bird targets mapped in PPI radar image are isolated gray spots with a congregated degree. This spatial characteristic could be fully studied to develop a new detection approach. Thereby, this difference can be applied to distinguish bird targets from background-edge clutter approximately by calculating the gray scale value in the neighborhood of the suspicious region shown as Fig. 3, in which N_{in} is the width of the suspicious region with central coordinates (i, j) and N_{out} is the width of the outside neighborhood. The method can be named neighborhood examination.

The mean gray scale value in the fringe part of Fig. 3 is calculated as

$$D(i,j,k) = \frac{\sum_{m=-N_{\text{out}}/2}^{N_{\text{out}}/2} \sum_{n=-N_{\text{out}}/2}^{N_{\text{out}}/2} G(i+m,j+n,k) - \sum_{m=-N_{in}/2}^{N_{in}/2} \sum_{n=-N_{in}/2}^{N_{in}/2} G(i+m,j+n,k)}{N_{\text{out}}^2 - N_{\text{in}}^2} \quad (1)$$

where $G(\cdot)$ represents the gray scale of the raw radar image; (i,j) = coordinates of bright pixels in the subtracted image; and k refers to the sampling instant. For edge clutter, many bright spots exist in the fringe part; otherwise, there exist few spot distributing around the target. A criteria is set to declare whether the target appears in the suspicious region by the indicator function shown as follows:

$$I(i,j,k) = \begin{cases} 1 & D(i,j,k) < S \\ 0 & \text{others} \end{cases} \quad (2)$$

where S = threshold. Not all the pixels in the raw image need to be examined, but only the bright pixels left in the subtracted image are concerned. In the context of target detection, the

Downloaded from ascelibrary.org by University of Science & Technology Beijing on 07/07/16. Copyright ASCE. For personal use only; all rights reserved.

neighborhood examination algorithm is performed at the pixels in the raw image with the locations of concerned pixels provided by the background-subtracted image.

Measurements Extraction

After the previous two steps, connected regions that exceed the detection threshold are presented as bright areas in the image whose information is extracted by region labeling and area measurement. The region labeling allows pixels of each disconnected target region in the binary PPI image to be labeled with the same number. On this basis, measurements including center coordinates (ρ, θ) and the size of each target represented by pixel number n are extracted. The polar coordinate system, whose origin is set in the center of the image, rotates counterclockwise.

Multitarget Tracking

Multitarget tracking in a cluttered environment can be divided into three parts: track initiation, track deletion, and track maintenance, according to different states of a target track. In this section, after birth events modeling track initiation and death events modeling track deletion, all possible associated events are enumerated in the track maintenance stage. The multitarget tracking algorithm will be tested subsequently against the simulated data.

Track Initiation

Track initiation is the first step for multitarget tracking. There are two main classes of track initiation approaches: sequential and batch techniques (He et al. 2006; Bar-shalom et al. 2001). The sequential techniques are usually considered to be appropriate for track initiation in the presence of a relatively uncluttered background. In the presence of heavy clutter, a batch technique is preferred. The tradeoff of using a batch technique is a heavier computational load and a slower process.

Heuristic and logic-based methods involve the processing of a sequence of measurements received during consecutive radar scans (Leung et al. 1996). Although the heuristic method uses two simple rules, namely velocity and acceleration constraints, to reduce potential tracks for initiation, the logic-based method uses prediction and gating to identify potential tracks in a multiple hypothesis fashion.

For the batch techniques, measurements from the past N scans are processed simultaneously to determine feasible target trajectories. The N scans of data are treated as an image, and the tracks are initiated if some curves (usually straight lines) are detected. Two of the most popular batch techniques are the Hough transform (HT) and its modified version (Chen et al. 1996). The standard HT, which uses the histogram approach, suffers from significant computational burden. Therefore, a modified HT technique is proposed to initiate a track by detecting "crossing" in the parameter space, which reduces the controlling parameter of the HT from two to one, and eliminates the use of a histogram. In our algorithm, the possibility of detection of a new potential target is modeled for track initiation. The probability of detecting a new target is equivalent to the probability of birth, which has the probability p_b (Särkkä et al. 2007). This modeling method can be regarded as a new branch in the sequential techniques.

Track Deletion

In multitarget tracking, the targets might escape from the surveillance region at any time, so timely resolution should be made to eliminate unwanted tracks, namely track deletion. Present multitarget track deletion techniques include sequential probability rate test, track gating, cost function, Bayes, and all-neighbor Bayes methods (He et al. 2006; Bar-shalom et al. 2001). All these techniques are based on the nearest neighbor algorithm and can be divided into two classes: recursive method based on targets and batch method based on measurements. The recursive method provides a light computational load but may be ineffective in a dense clutter environment. The batch method has a heavier computational load but works well in a dense clutter environment. In this algorithm, a death probability p_d that the target is dead at current time step is used for track deletion. The death probability of a target depends on the interval τ from the last association to the current time step. The relationship between the two variables is modeled as a gamma distribution (Särkkä et al. 2007)

$$p_d \sim \text{gamma}(\tau|\alpha,\beta) = \tau^{\alpha-1}\frac{\beta^{\alpha}e^{\frac{-\tau}{\beta}}}{\Gamma(\alpha)} \tag{3}$$

whose slope varies with variables α and β.

Track Maintenance

In a cluttered environment, considering birth and death events of targets, track maintenance is generally solved by data association method, on which much research has been done (He et al. 2006; Chen et al. 1996; Blackman 1999, 2004; Bar-Shalom et al. 2001). After data association, standard filtering technology (e.g., Kalman filtering) can be used for tracking. Methods for data association are typically divided into two classes: unique-neighbor data association [such as multiple hypothesis tracking (MHT)] and all-neighbor data association [such as joint probabilistic data association (JPDA)] (Blackman 2004; Kirubarajan and Bar-Shalom 2004). The main difference between them is that in the former, each measurement is associated with one of the previously created tracks, and in the latter, all measurements are used for updating all tracks. In MHT, each measurement is associated with an existing track, or a new track is formed according to the track initiation criterion. Instead of only one track configuration, several hypotheses are simultaneously formed and maintained as the data associations are not necessarily unique. Likelihoods of the measurements and the posterior hypotheses are calculated, and according to these only, the most probable hypotheses are stored.

In the track maintenance algorithm of this study, a particle filtering (PF) based data association method (Särkkä et al. 2007) is adopted, which can be considered as a generalization of MHT because every particle represents a different data association hypothesis. Event probability in each particle is calculated as

$$P = P_p \cdot P_l \tag{4}$$

where P_p = prior probability; and P_l = event associated likelihood depending on the measurements and current states of the existing targets. All possible associated events of measurements are then found as follows:

1. Clutter, no target dies

$$P_p = (1-p_b)\cdot(1-p_d)^n \cdot cp \qquad P_l = cd \tag{5}$$

   where cp = clutter prior; cd = clutter density value; n = target number at present; p_b = prior probability of birth; and p_d = death probability of the existing target.

2. Clutter, one target dies

$$P_p = \begin{cases} (1-p_b)\cdot p_d \cdot (1-p_d)^{n-1}\cdot cp & n>1 \\ (1-p_b)\cdot p_d \cdot cp & n=1 \end{cases} \qquad P_l = cd \tag{6}$$

J. Aerosp. Eng., 2012, 25(2): 246-255

Downloaded from ascelibrary.org by University of Science & Technology Beijing on 07/07/16. Copyright ASCE. For personal use only; all rights reserved.

3. Known target j, no target dies

$$P_p = (1 - p_b) \cdot (1 - p_d)^n \cdot (1 - cp)/n \qquad P_l = p_{\text{tlh}} \tag{7}$$

4. Known target j, one target dies

$$P_p = (1 - p_b) \cdot p_d \cdot (1 - p_d)^{n-1} \cdot (1 - cp)/(n - 1) \qquad n > 1$$
$$P_l = p_{\text{tlh}} \tag{8}$$

where p_{tlh} denotes the Kalman filter measurement likelihood evaluation with known targets.

5. New target, no target dies

$$P_p = p_b \cdot (1 - p_d)^n \qquad P_l = p_{\text{ilh}} \tag{9}$$

where p_{ilh} denotes the Kalman filter measurement likelihood evaluation with initial point.

6. New target, one target dies

$$P_p = \begin{cases} p_b \cdot p_d \cdot (1 - p_d)^{n-1} & n > 1 \\ p_b \cdot p_d & n = 1 \end{cases} \qquad P_l = p_{\text{ilh}} \tag{10}$$

After calculation of all event probabilities, the association result is determined by random selection method for each particle. Obviously, the event with higher probability will have more chances of selection as the association result. N particles are set with equal initial weights. $\{w_O^{(i)} = 1/N, i = 1, \ldots, N\}$. New weight of each particle is computed as

$$w_k^{(i)} = w_{k-1}^{(i)} \cdot P_l / P^* \tag{11}$$

where P^* = normalized value of P. Then, the weight is normalized and denoted as $w_k^{*(i)}$, and the effective number of particles is estimated as

$$n = \frac{1}{\sum_{i=1}^{N} (w_k^{*(i)})^2}. \tag{12}$$

If n is too low (e.g., $n < N/4$), resampling must be performed.

Track Smoothing

Target trajectories are smoothed by a Kalman smoother, which is also known as the Rauch-Tung-Striebel (RTS) smoother (Bar-Shalom et al. 2001). The difference between Kalman filtering and smoothing is that in Kalman filtering the recursion moves forward and in smoothing backward. In smoothing, the recursion starts from the last time step.

Data Overlay

Data overlay is the last step of the algorithm. In this study, the smoothed target trajectories are overlaid on a satellite map or coordinate system in real-time for observation, and are also recorded to a database for detailed postprocessing and further analysis. Ideally, GIS transformations can be applied during the track processing so that smoothed target tracks are located in earth coordinates, immediately suitable for display on maps downloaded from Google Earth.

Experiment Results Analysis

In this section, after testing the multitarget tracking algorithm against simulated data, the overall approach for PPI radar images are applied to a set of flying bird targets ground-truth data collected by BHEARS with horizontal scanning.

Simulated Experiments

The tracking algorithm's effectiveness is proven by tracking three targets with different birth and death times in two dimensions with cluttered measurements. The state of the target can be written as

$$\mathbf{m}_k = (x_k \quad y_k \quad \dot{x}_k \quad \dot{y}_k)^T$$

where (x_k, y_k) = target's position; and $(\dot{x}_k, \dot{y}_k)$ = velocity in two-dimensional Cartesian coordinates. Fig. 4 shows the trajectories of three targets. Target 1 starts from $(-2.5, 3)$ at 0 s, moves at the uniform speed of (1, 0) at 0–1.49 s, completes right turning at 1.50–4.0 s, moves at the uniform speed of $(0, -1)$ at 4.01–6.79 s, completes left turning at 6.8–9.3 s, moves at the uniform speed of (1, 0) at 9.31–10.0 s, and stops at 10.0 s. Target 2 starts from $(-2.5, 2)$ at 4.0 s, moves at the uniform speed of $(0, -1)$ at 4.0–5.49 s, completes left turning at 5.5–8.0 s, moves at the uniform speed of (1, 0) at 8.01–12.0 s, and stops at 12.0 s. Target 3 starts from $(-2, 2.5)$ at 6.0 s, moves at the uniform speed of $(1, -2.5)$ at 6.0–8.0 s, and stops at 8.0 s. Therefore, Target 1 exits alone during 0–4.0 s, Targets 1 and 2 exist together during 4.0–6.0 s; Targets 1, 2, and 3 exist together during 6.0–8.0 s; Targets 1 and 2 exist together during 8.0–10.0 s; and only Target 2 remains in 10.0–12.0 s. Target measurements are added with Gaussian noise, whereas other clutter measurements are uniformly distributed in space $[-4, 4] \times [-4, 4]$, and the clutter number in every scanning period matches with the λ-mean Poisson distribution.

In this study, 100 particles are used. λ is set at 0.1, p_b is set at 0.01, cp is set at 0.01, and cd is set at $1/64$. The target death model is defined with $\alpha = 2$ and $\beta = 0.4$. Real target tracks are shown with solid lines in Fig. 4, where target measurements are represented by ° and clutter measurements are represented by ×. The initial location of each target is circled. As it is shown in Fig. 5, the judgments on target birth and death time are in good agreement with true situations.

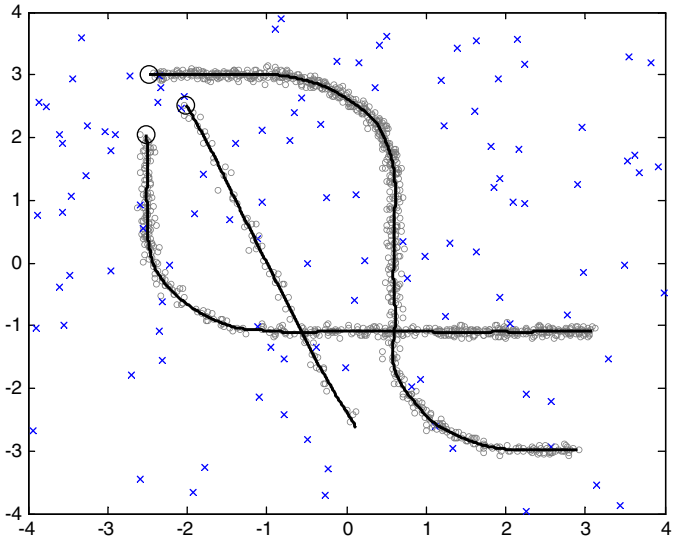

Fig. 4. Tracking simulation of three targets in clutter environment

Downloaded from ascelibrary.org by University of Science & Technology Beijing on 07/07/16. Copyright ASCE. For personal use only; all rights reserved.

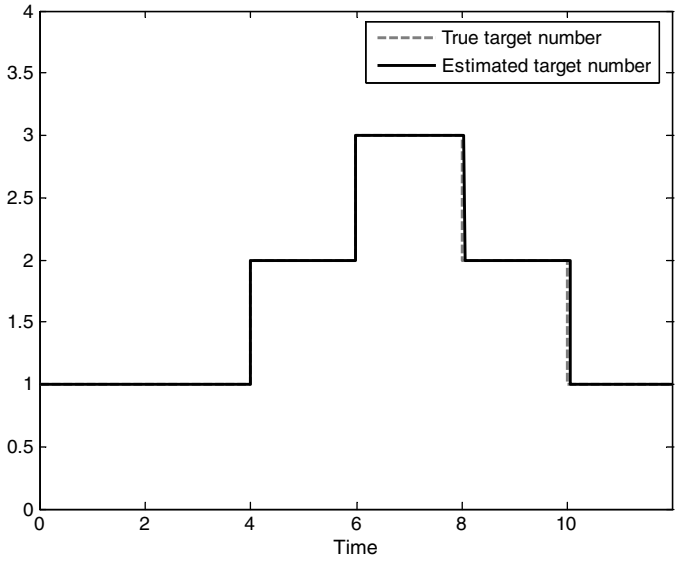

Fig. 5. Estimated target number in tracking simulation

Field Experiments

A sequence of 54 horizontal PPI images with a measurement range of 0.5 nmi was collected on the north bank of the Shahe Reservoir on September 29, 2007. The targets of interest were birds (wild ducks and swans) flying across the reservoir. Fig. 5 shows the whole processing of the 40th image of this sequence. Fig. 6(a) is raw radar image dominated by background attributed to buildings, trees, shoal, and dam in addition to the flying bird targets. After subtraction, Fig. 6(b) is obtained with most of the background removed but still large amounts of residual clutter left. Fig. 6(c) is the result by clutter suppression with threshold segmentation method, and Fig. 6(d) is the result by clutter suppression method with spatial characteristics proposed in this paper, when high bright regions in the image are our interesting areas. Radar measurements of the former method including polar coordinate positions (ρ, θ) and size n are extracted and presented in Table 1. The five suspicious regions are also labeled in Fig. 6(b). Measurements 4 and 5 clearly belong to background-edge clutter, which could be rejected by the clutter suppression method with spatial characteristics, so there are three measurements left (1, 2 and 3) in Fig. 6(d), which could reduce the burden of clutter rejection for tracking. For the detection mask, N_{in} is set at 21-pixel and N_{out} is set at 33-pixel. In the tracking step, a new track is initiated by using the birth model, and then, target measurements are selected and associated to the existing tracks to update their present states when clutter is rejected successfully. An old track is deleted when it has come to its end according to the death model.

The image sequence shows that three targets appear from start to finish: Target 1 appears in the images during the scanning period of 1–45 frames flying to the east; Target 2 appears at 27–42 frames flying to the southwest; and Target 3 appears from 37–54 frames flying to the southeast. After processing the whole sequence, the fusion image is shown as Fig. 6(e), in which a target is indicated by • in polar coordinates, and the smoothed trajectories are quite consistent with the observation. Measurements 1, 2 and 3 are flying birds, whose start and end points are given in Table 2. The number of existing targets varies during the 54 scanning periods, and the estimated result is shown in Fig. 7.

A sequence of vertical PPI radar images were collected during vertical scanning experiments on the north bank of Shahe Reservoir (Ning et al. 2010). The detection range of our system was set at 0.25 nmi, which exactly covered the north-south width of the reservoir. Compared with horizontal images, vertical images are easier to process because of less noise interference in the airspace. Therefore, the tracking module in the algorithm is omitted, and target positions are directly labeled in the height coordinate. The first quadrant of the PPI radar image, which represents the airspace above the water surface, is the concerned zone. The vertical axis shows the height distribution of the birds flying through the beam, whereas the horizontal axis represents their distances to the radar. For further investigation, with the target locations stored in the database over long periods of time, a map with flying bird height distribution is provided.

BASH Assessment

The BASH assessment is based on bird information extracted by the flying bird target detecting and tracking algorithm. First, a survey of related work is given. To improve the accuracy in estimating BASH, an analytic hierarchy process (AHP) was used to obtain values for weights of different elements. The BASH assessment technique was applied at Nanyang Airport.

Related Work

Different bird species pose different risks to aircraft because of their mass and number. At present, the general BASH assessment model uses the bird-strike data to estimate strike probabilities of different bird species. Allan (2006) created a simple probability-times-severity matrix to evaluate risk on the basis of both national and airport-specific data. The strike probability was measured by the frequency of strikes reported for different bird species at a given airport, whereas the likely severity was measured by the proportion of strikes with each species that result in damage to aircraft in the national bird-strike database. With reference to the protocol proposed by Allan, a tool is developed to provide decision-making support on the risk assessment process, by using a comprehensive database of Athens International Airport (Anagnostopoulos 2003). Shaw (2008) studied methods for evaluation of aircraft susceptibility to strike and bird specie's susceptibility to strike. The methods were successfully used at nine Australian airports. The United States Bird Avoidance Model (USBAM) has been established on the basis of the historical data accumulated in the database recording bird activities and bird strikes and combined with real-time information (Ruhe 2005). The USBAM is based on approximate 30 years of historical bird observation data, which are transformed into average bird mass values and interpolated spatially in a geographical information system environment with a resolution of 1 km^2. The BASH index is divided into nine levels according to bird distribution density per km^2. The China Academy of Civil Aviation Science and Technology has established the BASH Avoidance Information System for Civil Aviation of China, which is a data-sharing platform for the national avian situation management.

Common ground of the previous approaches is that the evaluation of the BASH probabilities of different bird species or aircraft type is always based on long-term stored reports on bird-strike events. However, there are few methods published to date for real-time BASH assessment depending on current states of flying birds and flights at airport. This article proposes an AHP-based scheme for real-time BASH assessment, which uses bird information collected by airport-based avian radar system and flight states of aircrafts provided by the air-traffic control (ATC) system. The

J. Aerosp. Eng., 2012, 25(2): 246-255

Downloaded from ascelibrary.org by University of Science & Technology Beijing on 07/07/16. Copyright ASCE. For personal use only; all rights reserved.

Downloaded from ascelibrary.org by University of Science & Technology Beijing on 07/07/16. Copyright ASCE. For personal use only; all rights reserved.

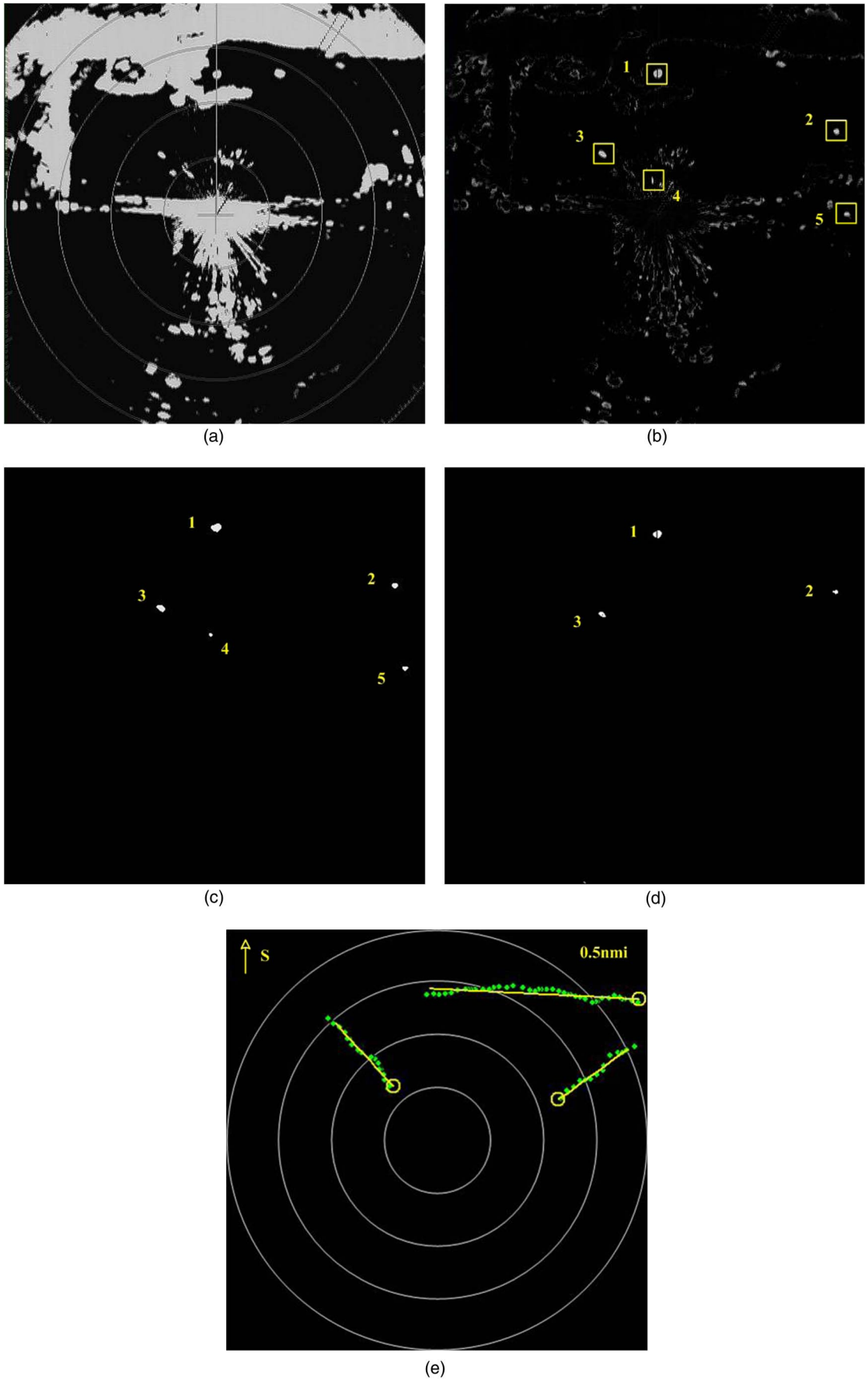

Fig. 6. Processing of horizontal PPI radar images: (a) raw PPI radar image; (b) PPI radar image after background subtraction; (c) PPI radar image after clutter suppression with threshold segmentation; (d) PPI radar image after clutter suppression with spatial characteristics; (e) fusion image with smoothing tracks

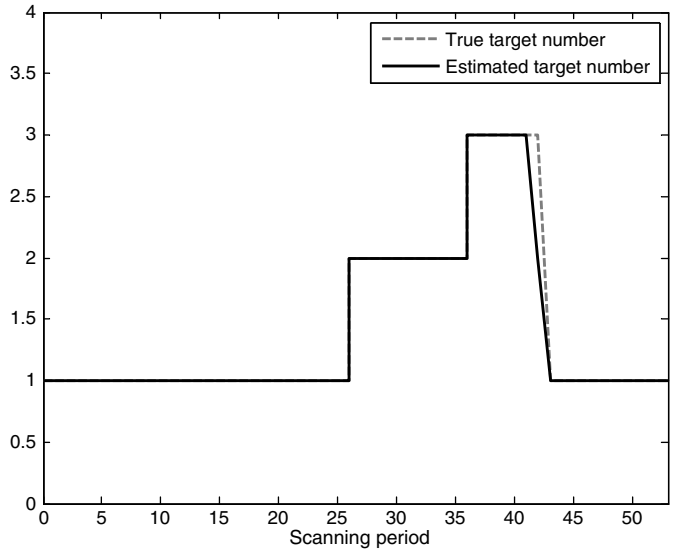

Fig. 7. Estimated target number for ground-truth data

airport personnel should take different actions to reduce the hazard according to different risk levels.

Using AHP in BASH Assessment

The AHP is based on the idea that a complex problem can be effectively examined if it is hierarchically decomposed into its components (Khorramshahgol and Djavanshir 2008). Thus, AHP provides a holistic view of the problem. AHP begins with the top level in the hierarchy that reflects the main objective. An element at a higher level of the hierarchy is said to be the governing element for those elements at the lower level. Elements at a certain level are compared against each other with reference to their effect on the governing element. Consider the elements $C_1, C_2, \ldots, C_n$ of some level in a hierarchy and denote their normalized weights by $w_1, w_2, \ldots, w_n$, respectively. The value of w_i reflects the degree of importance of the C_i with respect to the C_i governing element. The first step in the calculation of w_i is to derive pairwise comparisons between the n elements. These pairwise comparisons are structured into an $n \times n$ matrix called a comparison matrix

$$\mathbf{A} = \begin{bmatrix} C_1 & C_2 & \ldots & C_n \\ a(1,1) & a(1,2) & \ldots & a(1,n) \\ a(2,1) & a(2,2) & \ldots & a(2,n) \\ \vdots & \vdots & & \vdots \\ a(n,1) & a(n,2) & \ldots & a(n,n) \end{bmatrix} \begin{matrix} C_1 \\ C_2 \\ \vdots \\ C_n \end{matrix} \tag{13}$$

Elements of matrix $\mathbf{A}$ can be derived by using a nine-scale approach: $a(i,j) = 1$ if C_i and C_j are equally important; = 3 if C_i is weakly more important than C_j; = 5 if C_i is strongly more important than C_j; = 7 if C_i is very strongly more important than C_j; = 9 if C_i is absolutely more important than C_j; and = 2, 4, 6, 8 used to compromise between the two judgments. Also, $a(j,i) = 1/a(i,j)$ for all $j = 1, 2, \ldots, n$.

For BASH assessment at airports, four elements are introduced, including the number of birds N, the weight of birds W, the flying height of birds H, and the region in which birds appear at airports R. Therefore, the comparison matrix is given by ornithologists as follows (Wu 2006):

$$\mathbf{A} = \begin{bmatrix} N & W & H & R \\ 1 & 4 & 2 & 6 \\ 1/4 & 1 & 1/3 & 3 \\ 1/2 & 3 & 1 & 5 \\ 1/6 & 1/3 & 1/5 & 1 \end{bmatrix} \begin{matrix} N \\ W \\ H \\ R \end{matrix}$$

Weights of the four elements are calculated by an approximation technique; the weight of each element is the averaged and normalized value of all elements in its row. The four weights are as follows:

$$P_N = 0.564, \qquad P_W = 0.098, \qquad P_H = 0.304, \qquad P_R = 0.034$$

According to the specific situations at airports, scores of all elements are divided into n grades, and the BASH assessment index decided by bird information is calculated as follows:

$$T_{bird} = \frac{1}{n} \sum_{i=N,W,H,R} P_i \cdot G_i \tag{14}$$

where G_i denotes the grade division for each element. Beside the effects of bird information, flight state of aircraft is the other significant factor. Then, the double-factorial evaluation of the BASH assessment index is

$$T = T_{\text{bird}} \cdot T_{\text{flight}} \tag{15}$$

where T_{flight} is estimated based on the information provided by ATC system. T_{flight} can be endowed with different values between 0 and 1 according to different flight states. For instance, T_{flight} should be set at a higher value (e.g., 0.8–1.0) during the take-off or landing stage when the plane is more vulnerable to bird-strike or be set at a relatively lower value (e.g., < 0.5) when the plane is still at a long distance to airport or moving in the opposite direction of the birds. The hazard index is a value between 0 and 1, and can be divided into five grades represented by five colors to give increasing danger: blue ($0 \le T < 0.2$), green ($0.2 \le T < 0.4$), yellow ($0.4 \le T < 0.6$), orange ($0.6 \le T < 0.8$), and red ($0.8 \le T < 1$). Different measures should be taken by airport staff and pilots according to different alarm colors. When the color is blue or green, further observation should be made and informations transmitted to pilots without delay; when the color is yellow or orange, a professional bird-driven team should be sent and scheduled flights suspended; when the color is red, the involved airways should all be closed until the alarm is completely clear.

Table 1. Five Groups of Radar Measurements of Range, Angle, and Size

Number	ρ (m)	θ (°)	n
1	644.4	89.7	84
2	881.7	26.2	34
3	375.4	129.6	54
4	174.7	96.3	13
5	833.8	1.9	25

Table 2. Start and End Points of Radar Targets

	Start points		End points	
Number	ρ (m)	θ (°)	ρ (m)	θ (°)
1	1,065.9	34.4	642.2	94.1
2	567.4	19.1	957.8	25.5
3	308.4	133.5	718.7	131.7

J. Aerosp. Eng., 2012, 25(2): 246-255

Downloaded from ascelibrary.org by University of Science & Technology Beijing on 07/07/16. Copyright ASCE. For personal use only; all rights reserved.

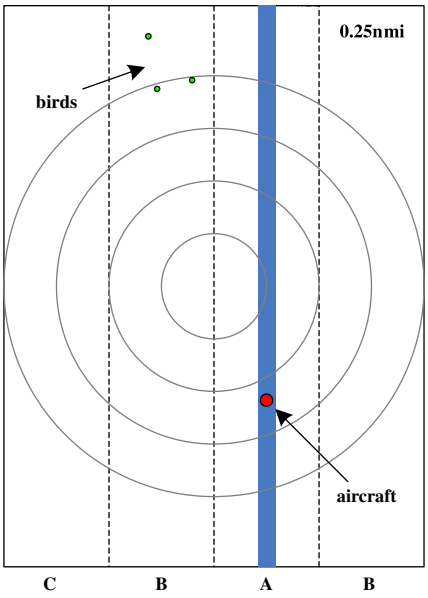

Fig. 8. Display of BHEARS at Nanyang Airport

Example Application

Experiments using BHEARS were carried out at Nanyang Airport on October 15, 2008. Fig. 8 presents the fusion image on the display at 17:45:32. An airplane from Beijing was landing, represented as a bigger dot in the image, whereas three birds are represented as small dots in the upper part of the figure. The specific rating standard to the four elements of the BASH assessment model are described in Table 3. The score of each element is divided into three grades.

Fig. 6 shows that Nanyang Airport is divided into three regions of A, B, and C. Region A is the runway and the areas beside it; Region B is the area next to region A; and other areas around the airport belong to Region C. By processing flying bird targets using the detecting and tracking algorithm, three birds (two small and one medium, discriminated by its size n) flying below the height of 150 m are detected in Region B. The accurate height of birds should be measured by vertical scanning radar; however, it is estimated by the horizontal scanning radar in this paper. Because the elevation beam width of our radar is 20° (10° upward above the ground) and the detection range is 500 m, the detected bird targets must be below the height of 150 m. Therefore, for Eq. (14), the score of number is set at 2, the score of weight is set at 2, the score of height is set at 3, and the score of region is set at 2, so the value of T_{bird} is 0.735. Meanwhile, T_{flight} is set at 0.85 because the aircraft was landing at that time. Therefore, the BASH assessment index is 0.625 calculated by Eq. (15), giving the orange-grade bird-aircraft strike alarm.

Table 3. Rating Standard to Elements of BASH Assessment Model at Nanyang Airport

Elements	Grade division	Score
Number (N)	$11 \sim 100$	3
	$2 \sim 10$	2
	1	1
Weight (W)	Large ($n > 100$)	3
	Medium ($50 \leq n \leq 100$)	2
	Small ($n < 50$)	1
Height (H)	$0 \sim 150$ m	3
	$151 \sim 600$ m	2
	$601 \sim 1{,}500$ m	1
Region (R)	A	3
	B	2
	C	1

Conclusions and Future Work

Throughout the development of an airport-based avian radar system, the system has become more and more intelligent and complicated, involving more technologies and subjects. However, two technologies are critical: first the flying bird target detecting and tracking algorithm and second the BASH assessment model.

A modern radar system usually contains a signal processor and a data processor. Signal processing performed in a signal processor includes Doppler filtering and space-time adaptive processing. Data processing typically operates on data after signal detection. The flying bird target detecting and tracking algorithm belongs to the work of the data processor. The radar adopted by BHEARS is a low-cost incoherent marine radar. The probabilities of detection and false alarms of the radar receiver are beyond the scope of this paper, and the authors would rather concentrate on a tracking algorithm based on the PPI images collected by the marine radar. For instance, if a bird flying through the radar beam was not detected and shown on radar monitor because of its low RCS and long distance, it is also impossible to be detected by this algorithm in data processing for the lack of data source.

The second technology needing research is data mining and modeling. In this paper, BASH is estimated by AHP based on two factors of flying birds and aircraft, giving a hazard index to indicate changes in safety or threat-level to aircraft. Four elements of birds, including number, weight, height, and region are considered. In the future, the authors will establish a more reasonable BASH assessment model in which the current states of birds and flight will be integrated into a multihierarchy structure in which the aircraft type will also be added as a factor. In addition, a Near-Miss Event (NME) index was recently proposed to detect changes in the probability of a bird-strike (Klope et al. 2009). The NME refers to birds and an aircraft passing within 50 m of one another. The dataset of NMEs can provide valuable information to aviation safety.

Otherwise, the design of the radar antenna is another major research issue. Most of the existing systems adopt a combination of two radars with array antennas. One scans horizontally and the other vertically. This configuration covers the airspace above the runway and the area around the airport but cannot give real 3D information. A new approach using multibeam technology has been developed by Accipiter, improving accuracy significantly, whereas maintaining coverage and controlling costs [P. Weber and T. J. Nohara, "Device & method for 3D height-finding avian radar," U.S. Patent No. 7864103 (2011)].

Research on an airport-based avian radar system is an interdisciplinary subject, covering study fields of ornithology, radar systems, image processing, multitarget detecting and tracking, and hazard assessment. The BHEARS, whose main technologies have been developed, is a platform in which further improvements and more advanced technologies will be applied in the future.

Acknowledgments

This work is jointly funded by the National Natural Science Foundation of China (NSFC) and Civil Aviation Administration

Downloaded from ascelibrary.org by University of Science & Technology Beijing on 07/07/16. Copyright ASCE. For personal use only; all rights reserved.

of China (CAAC) (No. 61079019 and No. 61001134). The authors also wish to acknowledge the support from the 47th China Postdoctoral Science Foundation and the Important National Science & Technology Specific Projects on the development and application validation of the next generation sensing network for civil airport perimeter anti-intrusion monitoring.

References

Allan, J. (2006). "A heuristic risk assessment technique for birdstrike management at airports." *Risk Anal.*, 26(3), 723–729.

Anagnostopoulos, A. (2003). "Bird strike risk assessment for Athens International Airport." *20th Int. Bird Strike Committee Conf.*, IBSC, Sand Hutton, York, UK.

Bar-Shalom, Y., Li, X. R., and Kirubarajan, T. (2001). *Estimation with applications to tracking and navigation*, Wiley, New York.

Beckwith, R. A. (2005). "Radar video processing systems." Curtiss-Wright Controls Embedded Computing, Letchworth, Garden City, UK.

Blackman, S. S. (2004). "Multiple hypothesis tracking for multiple target tracking." *IEEE Aerosp. Electron. Syst. Mag.*, 19(1–2), 5–18.

Blackman, S. S., and Popoli, R. (1999). *Design and analysis of modern tracking systems*, Artech House, Boston.

Chen, J., Leung, H., Lo, T. et al. (1996). "A modified probabilistic data association filter in a real clutter environment." *IEEE Trans. Aerosp. Electron. Syst.*, 32(1), 300–313.

He, Y., Xiu, J. J., Zhang, J. W., and Guan, X. (2006). *Radar data processing with applications*, Publishing House of Electronics Industry, Beijing.

Khorramshahgol, R., and Djavanshir, G. R. (2008). "The application of analytic hierarchy process to determine proportionality constant of the taguchi quality loss function." *IEEE Trans. Eng. Manage.*, 55(2), 340–348.

Kirubarajan, T., and Bar-Shalom, Y. (2004). "Probabilistic data association techniques for target tracking in clutter." *Proc. IEEE*, 92(3), 536–557.

Klope, M. W., Beason, R. C., Nohara, T. J., and Begier, M. J. (2009). "Role of near-miss bird strikes in assessing hazards." *Human-Wildlife Conflicts*, 3(2), 208–216.

Leung, H., Hu, Z., and Blanchette, M. (1996). "Evaluation of multiple target track initiation techniques in real radar tracking environments." *IEE Proc.—Radar, Sonar, Navig.*, 143(4), 246–254.

Ning, H. S., Chen, W. S., Mao, X., and Li, J. (2010). "Bird-aircraft strike avoidance radar." *IEEE Aerosp. Electron. Syst. Mag.*, 25(1), 19–28.

Nohara, T. J. (2009a). "Could avian radar have prevented US Airways Flight 1549's bird strike?" *Bird Strike North American Conf.*, Bird Strike Committee USA, 14–17.

Nohara, T. J. (2009b). "Reducing bird strikes: new radar networks can help make skies safer." *J. Air Traffic Control*, 51(3), 25–32.

Nohara, T. J., Unkrainec, W. A. et al. (2007). "An overview of avian radar developments—Past, present and future." *Bird Strike North American Conf.*, Bird Strike Committee USA, Sandusky, OH, 10–13.

Ruhe, W. (2005). "Bird avoidance models vs. real time bird-strike warning systems—A comparison." International Bird Strike Committee, Sand Hutton, York, UK, 195–200.

Särkkä, S., Vehtari, A., and Lampinen, J. (2007). "Rao-Blackwellized particle filter for multiple target tracking." *Inf. Fusion*, 8(1), 2–15.

Shaw, P., and McKee, J. (2008). "Risk assessment: Quatifying aircraft and bird susceptibility to strike." Int. Bird Strike Committee, Sand Hutton, York, UK, 24–28.

Wu, Qi (2006). "Study on prevention and control strategy of bird strike at the airport and design and realization of the birdstrike safety's assessment system." M.S., thesis, East China Normal Univ., Shanghai, China.

Downloaded from ascelibrary.org by University of Science & Technology Beijing on 07/07/16. Copyright ASCE. For personal use only; all rights reserved.